Biochemical and Biophysical Research Communications 428 (2012) 458–462

Contents lists available at SciVerse ScienceDirect

Biochemical and Biophysical Research Communications

journal homepage: www.elsevier.com/locate/ybbrc

Solid-state NMR analysis of the β-strand orientation of the protofibrils of amyloid β-protein

Takashi Doi [a], Yuichi Masuda [a,b,*], Kazuhiro Irie [c], Ken-ichi Akagi [d], Youko Monobe [d], Takayoshi Imazawa [d], K. Takegoshi [a]

[a] Graduate School of Science, Kyoto University, Kyoto 606-8502, Japan
[b] Graduate School of Pharmaceutical Sciences, Tohoku University, Sendai 980-8578, Japan
[c] Graduate School of Agriculture, Kyoto University, Kyoto 606-8502, Japan
[d] Section of Laboratory Equipment, Division of Biomedical Research, National Institute of Biomedical Innovation, Osaka 567-0085, Japan

ARTICLE INFO

Article history:
Received 29 September 2012
Available online 3 November 2012

Keywords:
Alzheimer's disease
Amyloid β-protein
Protofibrils
Solid-state NMR
Rotational resonance

ABSTRACT

Alzheimer's disease (AD) is caused by abnormal deposition (fibrillation) of a 42-residue amyloid β-protein (Aβ42) in the brain. During the process of fibrillation, the Aβ42 takes the form of protofibrils with strong neurotoxicity, and is thus believed to play a crucial role in the pathogenesis of AD. To elucidate the supramolecular structure of the Aβ42 protofibrils, the intermolecular proximity of the Ala-21 residues in the Aβ42 protofibrils was analyzed by ^{13}C–^{13}C rotational resonance experiments in the solid state. Unlike the Aβ42 fibrils, an intermolecular ^{13}C–^{13}C correlation was not found in the Aβ42 protofibrils. This result suggests that the β-strands of the Aβ42 protofibrils are not in an in-register parallel orientation. Aβ42 monomers would assemble to form protofibrils with the β-strand conformation, then transform into fibrils by forming intermolecular parallel β-sheets.

1. Introduction

A major pathological hallmark of Alzheimer's disease (AD) is the formation of senile plaque (SP) in the brain cortex [1]. SP is mainly composed of deposits of 39–43 residue amyloid β-proteins (Aβ39–43) [2,3], which are generated by the proteolytic cleavage of amyloid precursor proteins by β- and γ-secretases [4,5]. The major species in Aβ production are Aβ40 and Aβ42; Aβ42 is far more aggregative and neurotoxic [6], and is predominant in SP [7]. Aβ monomers first assemble to form low-number oligomers, and then accumulate into protofibrils: soluble short fibers. The resultant protofibrils ultimately transform into mature fibrils. It has been shown that Aβ oligomers show stronger neurotoxicity than the mature fibrils [8] and cause synaptic dysfunction [9]. It is thus useful and helpful for the prevention and drug development of AD to investigate the oligomerization mechanism of Aβ42. However, the structural analysis of Aβ oligomers is very difficult, because they are usually unstable and aggregative in aqueous solution.

Solid-state nuclear magnetic resonance (NMR) is a powerful method for analyzing not only the mature fibrils, but also the unstable oligomers, because frozen and freeze-dried protein samples are applicable. Several groups recently succeeded in preparing stable Aβ oligomers and analyzed their structures using solid-state NMR. Chimon et al. prepared spherical Aβ40 oligomers at 4 °C and revealed the existence of intermolecular in-register parallel β-sheets [10]. Ahmed et al. reported that disk-shaped oligomers of Aβ42 prepared at 4 °C mainly consisted of pentamers that do not form in-register parallel β-sheets [11]. Scheidt et al. prepared stable protofibrils of Aβ40 at 37 °C using an antibody as a fibrillation inhibitor and analyzed their secondary structures [12]. As described above, the temperature and use of additives drastically affects the size and structure of the Aβ oligomers. Therefore, to elucidate the structure of the Aβ42 oligomers under as close to physiological conditions as possible, we prepared Aβ42 protofibrils at 37 °C without any additive and analyzed their supramolecular structure using solid-state NMR.

2. Materials and methods

2.1. General

The following spectroscopic and analytical instruments were used: superconducting magnet for NMR, JASTEC 14.1 T

Abbreviations: AD, Alzheimer's disease; Aβ, amyloid β; SP, senile plaque; NMR, nuclear magnetic resonance; HPLC, high performance liquid chromatography; MALDI-TOF-MS, matrix-assisted laser desorption/ionization time-of flight mass spectroscopy; FAB-MS, fast atom bombardment mass spectroscopy; RP-HPLC, reversed-phase HPLC; SEC, size exclusion chromatography; CP, cross polarization; MAS, magic angle spinning; RAMP-CP, ramped-amplitude CP; TPPM, two pulse phase-modulated; R2, rotational resonance.

* Corresponding author. Address: Graduate School of Pharmaceutical Sciences, Tohoku University, 6-3 Aza-Aoba, Aramaki, Aoba-ku, Sendai 980-8578, Japan. Fax: +81 22 795 6864.
E-mail address: masuda@mail.pharm.tohoku.ac.jp (Y. Masuda).

0006-291X/$ - see front matter © 2012 Elsevier Inc. All rights reserved.
http://dx.doi.org/10.1016/j.bbrc.2012.10.096

superconducting magnet (JASTEC, Hyogo, Japan); solid-state NMR spectrometer, JEOL ECA600 spectrometer; solid-state NMR probe, a custom-fabricated probe with a Chemagnetics 3.2 mm spinning system; peptide synthesizer, Pioneer™ peptide synthesizer (Applied Biosystems, Foster City, CA); HPLC, Waters 600E multisolvent delivery system with a 2487 UV dual λ absorbance detector (Milford, MA); matrix-assisted laser desorption/ionization time-of flight mass spectroscopy (MALDI-TOF-MS), 4700 Proteomics analyzer (Applied Biosystems); transmission electron microscope, H-7650 (Hitachi High-Technologies, Ibaraki, Japan). HPLC was carried out on a Develosil-packed column ODS-UG-5 (20-mm inner diameter × 150 mm) (Nomura Chemicals, Seto, Japan). HiLoad 16/600 Superdex 75 pg (GE Healthcare, Japan) was used for size exclusion chromatography (SEC).

L-Alanine ($^{13}C{=}O$) and L-alanine ($^{13}C_\alpha$) were purchased from Taiyo Nippon Sanso Corporation (Tokyo, Japan). HATU [13] and *N*-α-(9-fluorenylmethoxycarbonil) (Fmoc) amino acids, *p*-alkoxybenzyl alcohol polyethylene glycol-polystyrene support (PAC-PEG-PS) resin were from Applied Biosystems.

2.2. Preparation of protected amino acids labeled with ^{13}C

Fmoc derivatives of L-alanine ($^{13}C{=}O$) and L-alanine ($^{13}C_\alpha$) were synthesized as reported previously [14]. The structures were confirmed by ^1H NMR, ^{13}C NMR, and FAB-MS measurements.

2.3. Synthesis of Aβ42 peptide labeled with ^{13}C

Peptide synthesis was performed in a stepwise manner on 0.1 mmol of Fmoc-Ala-PEG-PS resin by the Pioneer™ instrument with the Fmoc method using HATU [13], as reported previously [15–17]. For the synthesis of an equal mixture of Aβ42 labeled at C=O of Ala-21 and that labeled at C_α of Ala-21 with ^{13}C (Supplementary Fig. S1), the Fmoc amino acid at Ala-21 was applied as an equal mixture of *N*-Fmoc-L-alanine ($^{13}C{=}O$) and *N*-Fmoc-L-alanine ($^{13}C_\alpha$). The obtained crude peptide was purified by RP-HPLC using the Develosil packed column (20 mm inner diameter × 150 mm) with elution at 8.0 mL/min by an 80 min linear gradient of 10–50% CH_3CN including 0.1% NH_4OH as previously reported [16]. Lyophilization gave the corresponding pure Aβ peptide (10% yield), whose purity was confirmed by HPLC (>98%). The synthesized peptide exhibited satisfactory mass spectral data by MALDI-TOF-MS (Supplementary Fig. S3) for an equal mixture of Aβ42 labeled at C=O of Ala-21 and that labeled at C_α of Ala-21 with ^{13}C (MH^+, average molecular mass; observed 4515.99, calculated 4516.11) .

2.4. Preparation of the protofibrils and the fibrils of Aβ42

Purified Aβ42 peptide was dissolved in 0.1% NH_4OH at 1 mM. After a 10-fold dilution with 50 mM CH_3COONH_4 aqueous solution (pH 5.6), the resulting peptide solution (100 μM, pH 7.4) was incubated at 37 °C under a quiescent condition. After 5 h incubation, the mixture was centrifuged at 20,630*g* and 4 °C, and the supernatant was applied to SEC. The condition of SEC was; column, HiLoad 16/600 Superdex 75 pg (purchased from GE Healthcare Japan); eluting solvent, 50 mM CH_3COONH_4 aqueous solution (pH 7.4); flow rate, 0.6 mL/min. The molecular weight of Aβ42 protofibrils may be more than 70 kDa because the Aβ42 protofibrils were eluted at void volume. The fraction containing protofibrils (Supplementary Fig. S2) was rapidly frozen in liquid nitrogen and lyophilized. For the preparation of the Aβ42 fibrils, the Aβ42 solution (100 μM, pH 7.4) in 50 mM CH_3COONH_4 was incubated at 37 °C under a quiescent condition for 48 h. After centrifugation at 20,630*g* and 4 °C, the resulting pellets were lyophilized. The amount of obtained powder samples was; the Aβ42 protofibrils, 2.6 mg (17% yield from the Aβ42 monomers); the Aβ42 fibrils, 1.9 mg (95% yield from the Aβ42 monomers).

2.5. Transmission electron microscopy of negatively stained preparations of the protofibrils and the fibrils of Aβ42

The protofibrils and the fibrils of Aβ42 were prepared in the same conditions as those used for preparing the solid-state NMR samples. The SEC fraction of the Aβ42 protofibrils and the suspension of the Aβ42 fibrils before lyophilization were applied to 200-mesh Formvar-coated copper grids (Nissin EM, Tokyo, Japan) and dried in air before being negatively stained for a few seconds with 2% uranyl acetate. The morphologies (Fig. 1) were examined with the HITACHI H-7650 transmission electron microscope.

2.6. Solid-state NMR experiments

All solid-state NMR experiments were carried out at 14.1 T (150 MHz for ^{13}C) using a JEOL ECA600 spectrometer and a custom-fabricated probe with a Chemagnetics 3.2 mm spinning system at room temperature. The ^{13}C chemical shifts were calibrated in ppm relative to TMS by taking the ^{13}C chemical shift for the methine carbon nucleus of solid adamantine (29.5 ppm) as an external reference standard [18].

Pulse sequence parameters for ^{13}C 1D CP/MAS experiments were: MAS speed = 15 kHz, ramped-amplitude CP (RAMP-CP) contact time = 1 ms, pulse delay = 2 s, two pulse phase-modulated (TPPM) ^1H decoupling power = 80 kHz, dwell time = 33 μs and number of acquisition = 20,480. Background suppression pulse [19] was used to suppress background signals from the MAS module.

For the estimation of ^{13}C–^{13}C distance, ^{13}C 1D Rotational Resonance (R2) experiments [20] were used, whose pulse sequence were shown in Fig. 2. Pulse sequence parameters for R2 experiments were: MAS speed = 18,800 Hz, RAMP-CP contact time = 1 ms, pulse delay = 2 s, TPPM ^1H decoupling power = 80 kHz, dwell time = 19 μs, chemical shift filter interval (τ_f) = 10.5 μs, mixing time (τ_m) = 0.5–100 ms and number of acquisition = 20,000. The chemical shift filter interval (τ_f = 10.5 μs) was experimentally determined in order to eliminate $^{13}C_\alpha$ signal completely.

3. Results and discussion

3.1. Preparation of the Aβ42 protofibrils labeled with ^{13}C

Intermolecular in-register parallel β-sheets play a crucial role in the fibrillation of many aggregative proteins, such as Aβ, α-synuclein, and β_2-microglobulin [21]. Although the mature fibrils of Aβ42 have been demonstrated to form intermolecular in-register parallel β-sheets, it has not yet been clarified whether the Aβ42 protofibrils also form the same structure. Because Ala-21 in the Aβ42 fibrils is included in the β-sheets [22,23], the intermolecular proximity of the Ala-21 residues of the Aβ42 protofibrils was measured using solid-state NMR. To solely and accurately detect the intermolecular dipole–dipole interaction, an equal mixture of Aβ42 labeled with ^{13}C at the C=O and at C_α of Ala-21 was prepared (Supplementary Fig. S1). The Aβ42 protofibrils were synthesized following Walsh's protocol, in which the Aβ42 protofibrils were formed at 37 °C and separated by size exclusion chromatography (SEC) [24]. The Aβ42 monomers, low-number oligomers, protofibrils, and fibrils are in equilibrium. It was found that the amount of protofibrils was relatively large after incubation for ca. 5 h at 37 °C (Supplementary Fig. S2). The mature fibrils were removed by centrifugation, and the supernatant was subjected to

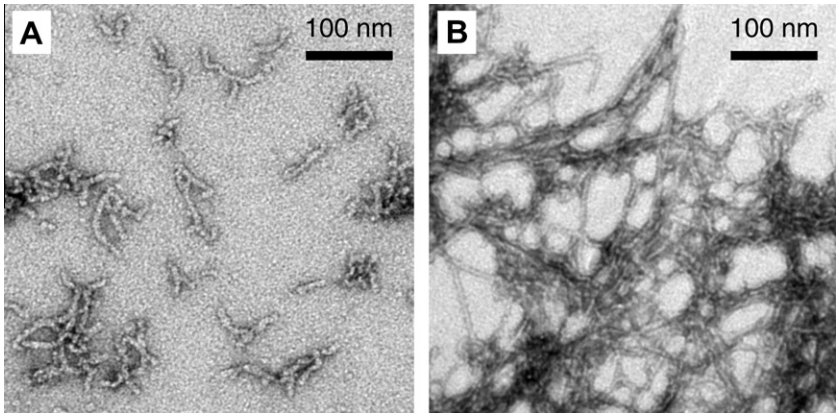

Fig. 1. Transmission electron micrographs of negatively stained preparations of Aβ42 protofibrils (A) and fibrils (B).

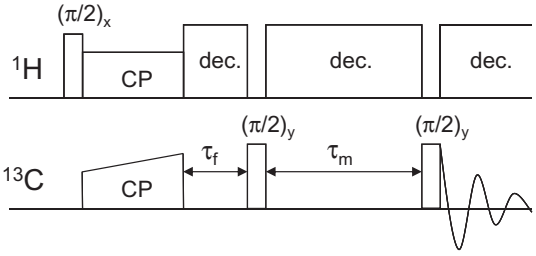

Fig. 2. A pulse sequence of the ^{13}C 1D R2 experiment with a chemical shift filter.

SEC. The fraction including the Aβ42 protofibrils was quickly frozen in liquid nitrogen and freeze-dried. Lyophilization with a typical buffer gave a large amount of salts and very little protein in the powder sample. To solve this problem, an ammonium acetate solution was used as the solvent because it is volatile. For comparison, the sediment including the mature fibrils was also dried *in vacuo*.

3.2. Transmission electron microscopy

The morphology of each sample was evaluated using transmission electron microscopy (TEM) (Fig. 1). In the solution of the Aβ42 protofibrils (Fig. 1A), small fibers (diameter of approximately 10 nm and length of approximately 100 nm) were observed. The morphology was apparently different from that of Aβ42 fibrils, which exist as a mass of long fibers that are intricately entangled (Fig. 1B). The morphology of our protofibrils is very similar to those of Scheidt's and Walsh's groups, which were prepared at 37 °C [12,24]. On the other hand, Chimon et al. and Ahmed et al. previously observed spherical or disk-shaped oligomers after incubation at 4 °C [10,11]. These differences indicate that temperature has a great influence on the morphology of the Aβ oligomers; protofibrils were formed at 37 °C and round-shaped oligomers at 4 °C. In fact, Ahmed et al. also observed protofibrils when Aβ42 was incubated at 37 °C [11].

3.3. Solid-state NMR analysis

The ^{13}C 1D spectra of the fibrils and the protofibrils were obtained using the cross polarization and magic angle spinning (CP/MAS) method. The 1D spectrum of each sample gave two significant peaks: $^{13}C{=}O$ and $^{13}C_\alpha$ in Ala-21. The line-widths of the peaks for the protofibrils are larger than those for the fibrils (Fig. 3A and E, and Supplementary Table S1). Deviations of the ^{13}C chemical shifts in the peptides relative to those of their corresponding random coils ($\Delta\delta = \delta_{observed} - \delta_{random\ coil}$) correlate with the secondary

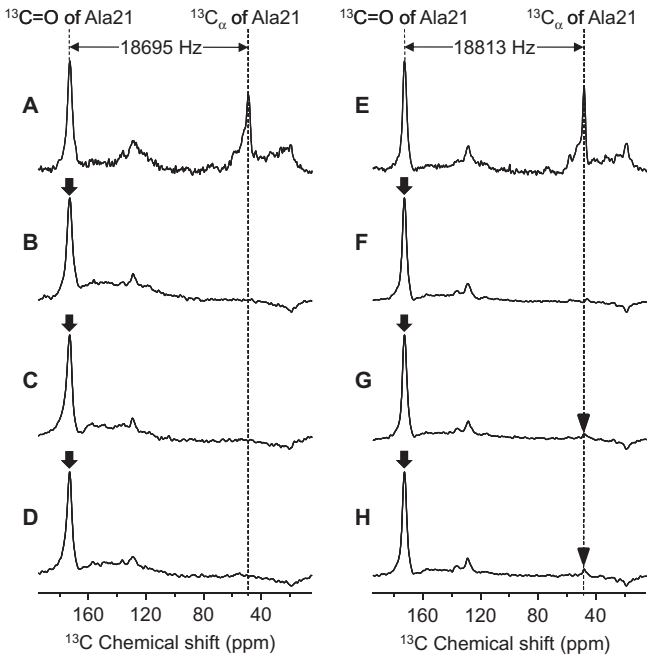

Fig. 3. 1D ^{13}C CP/MAS (A and E) and 1D R2 (B–D and F–H) spectra. The samples include the protofibrils (A–D) and fibrils (E–H) of an equal mixture of Aβ42 labeled with ^{13}C at the C=O and C_α of the Ala-21. The mixing times were 0.5 ms (B and F), 50 ms (C and G), and 100 ms (D and H). The broad signals around δ 120–130 ppm and δ 20–40 ppm were derived from the naturally abundant ^{13}C in Aβ42. Intermolecular magnetization transfer from the $^{13}C{=}O$ (arrow) to the $^{13}C_\alpha$ (arrowhead) due to the R2 effect was detected only in the fibrils.

structure. Wishart et al. reported that the $\Delta\delta$ of the $^{13}C_\alpha$ is positive in α-helices and negative in β-sheets [25]. The $\Delta\delta$ of $^{13}C_\alpha$ for the protofibrils ($\Delta\delta = -1.7$ ppm) is negative, but the difference is smaller than that for the fibrils ($\Delta\delta = -2.4$ ppm). The data on the line-widths and the secondary shifts, therefore, suggest that Ala-21 of the Aβ42 protofibrils is included in the β-strand, but could be less ordered than the Ala-21 in the Aβ42 fibrils.

To analyze the supramolecular structure, rotational resonance (R2) experiments were performed [20]. In this experiment, the MAS speed was adjusted to the difference between the chemical shifts of the two ^{13}C spins of interest (the R2 condition). Under the R2 condition, the magnetization transfer within the ^{13}C spins is driven by the reintroduction of the dipole–dipole interaction. It has been reported that ^{13}C dipole–dipole interactions of two ^{13}C spins within 6 Å can generally be recoupled by R2 [26–28]. According to the structural model of ^{35MOX}Aβ42 fibrils reported by Lührs

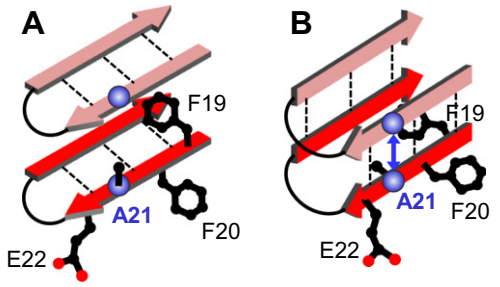

Fig. 4. (A) Possible structure of Aβ protofibrils with intramolecular antiparallel β-sheets, as proposed by Scheidt et al. [32]. (B) Molecular structure of Aβ fibrils with intermolecular parallel β-sheets, as demonstrated by Tycko and colleagues [22]. Dotted lines indicate hydrogen bonds. A blue double-headed arrow shows observed dipole–dipole interaction. (For interpretation of the references to color in this figure legend, the reader is referred to the web version of this article.)

et al. [29], the intermolecular distance between C=O and C_α of Ala-21 in the intermolecular parallel β-sheet could be 4.3–5.3 Å. In order to detect the magnetization transfer with high sensitivity, the $^{13}C_\alpha$ magnetization was made invisible using the chemical-shift difference between the ^{13}C=O and the $^{13}C_\alpha$, and the movement of the magnetization from the ^{13}C=O to the $^{13}C_\alpha$ during the mixing time was observed (Fig. 2). The intermolecular distance between the ^{13}C=O and $^{13}C_\alpha$ in the Ala-21 of E22K-Aβ42 (Italian) fibrils has previously been achieved by us using this method [14].

In the ^{13}C 1D R2 experiment with the Aβ42 fibrils (Fig. 3F–H), the $^{13}C_\alpha$ signal was recovered and increased in proportion to the mixing time. Because only one of the carbons (the C=O or C_α) in the Ala-21 is selectively ^{13}C-labeled, the intramolecular magnetization transfer is negligible. Therefore, the recovery of C_α due to R2 recoupling suggests that the intermolecular distance between the ^{13}C=O and $^{13}C_\alpha$ in the Ala-21 is within 6 Å. These results correspond to previous reports that the Ala-21 of Aβ42 fibrils forms intermolecular in-register parallel β-sheets [22,23]. On the other hand, in the ^{13}C 1D R2 experiment with the Aβ42 protofibrils (Fig. 3B–D), no significant peak for $^{13}C_\alpha$ was observed, even with a mixing time of 100 ms. This result indicates that the intermolecular distance between the ^{13}C=O and $^{13}C_\alpha$ in the Ala-21 is not within 6 Å, and that the β-strands of the protofibrils are not in an in-register parallel orientation. We also performed the R2 experiment between ^{13}C=O and $^{13}C_\alpha$ of the Ala-21 in the Aβ42 monomers, in which the distance should be far from each other. Expectedly, we did not observe the intermolecular dipole–dipole interaction in the Aβ42 monomers (Supplementary Fig. S4), supporting that magnetization transfer between distant carbons cannot be detected by our R2 method.

Härd and colleagues previously indicated that Aβ oligomers form intramolecular antiparallel β-sheet at positions 17–36 [30,31]. Quite recently, Scheidt et al. suggested that Aβ40 protofibrils also form intramolecular antiparallel β-sheets similar to Aβ oligomers (Fig. 4A) [32]. These data implied that conversion of intramolecular antiparallel β-sheets (Fig. 4A) into intermolecular parallel β-sheets (Fig. 4B) could occur on the pathway from protofibrils to mature fibrils [32]. In this study, an intermolecular proximity was observed between the Ala-21 residues in the Aβ42 fibrils, but not between those in the Aβ42 protofibrils. The present data is consistent with the aggregation model suggested by Scheidt et al. [32], because the intermolecular distance of the Ala-21 in the Aβ42 protofibrils could be long due to the steric hindrance of the side chains (Fig. 4A), where the distance between two β-sheets could be ~10.7 Å based on the X-ray fiber diffraction [33]. In contrast, the intermolecular distance of the C=O and C_α in the Ala-21 could be proximal in the Aβ42 fibrils, because the main chains are connected through hydrogen bonding (Fig. 4B). It is surprising that drastic reorientation of the β-strands would occur when the protofibrils transform into the fibrils despite the similarity in their fiber structures. A more detailed analysis of the intermolecular contacts between Aβ molecules in protofibrils is currently under investigation.

Acknowledgments

We thank Dr. H. Fukuda at Theravalues Corporation for the MALDI-TOF-MS measurements. This research was supported in part by the Promotion of Science for Young Scientists (Grant No. 21.1128 to Y.M.), Grant-in-aid for Scientific Research (A) (Grant No. 21248015 to K.I.), and the Global COE Program "International Center for Integrated Research and Advanced Education in Materials Science" (No. B-024) of the Ministry of Education, Culture, Sports, Science and Technology (MEXT) of Japan, administrated by the Japan Society for the Promotion Science.

Appendix A. Supplementary data

Supplementary data associated with this article can be found, in the online version, at http://dx.doi.org/10.1016/j.bbrc.2012.10.096.

References

[1] D.J. Selkoe, Alzheimer's disease: genes, proteins, and therapy, Physiol. Rev. 81 (2001) 741–766.
[2] G.G. Glenner, C.W. Wong, Alzheimer's disease: initial report of the purification and characterization of a novel cerebrovascular amyloid protein, Biochem. Biophys. Res. Commun. 120 (1984) 885–890.
[3] C.L. Masters, G. Simms, N.A. Weinman, G. Multhaup, B.L. McDonald, K. Beyreuther, Amyloid plaque core protein in Alzheimer disease and Down syndrome, Proc. Natl. Acad. Sci. USA 82 (1985) 4245–4249.
[4] J. Kang, H.G. Lemaire, A. Unterbeck, J.M. Salbaum, C.L. Masters, K.H. Grzeschik, G. Multhaup, K. Beyreuther, B. Müller-Hill, The precursor of Alzheimer's disease amyloid A4 protein resembles a cell-surface receptor, Nature 325 (1987) 733–736.
[5] K.S. Vetrivel, G. Thinakaran, Amyloidogenic processing of β-amyloid precursor protein in intracellular compartments, Neurology 66 (2006) S69–73.
[6] J.T. Jarrett, E.P. Berger, P.T. Lansbury Jr., The carboxy terminus of the β amyloid protein is critical for the seeding of amyloid formation: implications for the pathogenesis of Alzheimer's disease, Biochemistry 32 (1993) 4693–4697.
[7] A.E. Roher, J.D. Lowerson, S. Clarke, A.S. Woods, R.J. Cotter, E. Gowing, M.J. Ball, β-Amyloid-(1–42) is a major component of cerebrovascular amyloid deposits: implications for the pathology of Alzheimer disease, Proc. Natl. Acad. Sci. USA 90 (1993) 10836–10840.
[8] C.G. Glabe, Common mechanisms of amyloid oligomer pathogenesis in degenerative disease, Neurobiol. Aging 27 (2006) 570–575.
[9] C. Haass, D.J. Selkoe, Soluble protein oligomers in neurodegeneration: lessons from the Alzheimer's amyloid β-peptide, Nat. Rev. Mol. Cell Biol. 8 (2007) 101–112.
[10] S. Chimon, M.A. Shaibat, C.R. Jones, D.C. Calero, B. Aizezi, Y. Ishii, Evidence of fibril-like β-sheet structures in a neurotoxic amyloid intermediate of Alzheimer's β-amyloid, Nat. Struct. Mol. Biol. 14 (2007) 1157–1164.
[11] M. Ahmed, J. Davis, D. Aucoin, T. Sato, S. Ahuja, S. Aimoto, J.I. Elliott, W.E.V. Nostrand, S.O. Smith, Structural conversion of neurotoxic amyloid-β(1–42) oligomers to fibrils, Nat. Struct. Mol. Biol. 17 (2010) 561–568.
[12] H.A. Scheidt, I. Morgado, S. Rothemund, D. Huster, M. Fändrich, Solid-state NMR spectroscopic investigation of Aβ protofibrils: implication of a β-sheet remodeling upon maturation into terminal amyloid fibrils, Angew. Chem. 123 (2011) 2889–2892. Angew. Chem. Int. Ed. 50 (2011) 2837–2840.
[13] L.A. Carpino, 1-Hydroxy-7-azabenzotriazole. An efficient peptide coupling additive, J. Am. Chem. Soc. 115 (1993) 4397–4398.
[14] Y. Masuda, A. Nakanishi, R. Ohashi, K. Takegoshi, T. Shimizu, T. Shirasawa, K. Irie, Verification of the intermolecular parallel β-sheet in E22K-Aβ42 aggregates by solid-state NMR using rotational resonance. implications for the supramolecular arrangement of the toxic conformer of Aβ42, Biosci. Biotechnol. Biochem. 72 (2008) 2170–2175.
[15] K. Irie, K. Oie, A. Nakahara, Y. Yanai, H. Ohigashi, P.A. Wender, H. Fukuda, H. Konishi, U. Kikkawa, Molecular basis for protein kinase C isozyme-selective binding: the synthesis, folding, and phorbol ester binding of the cysteine-rich domains of all protein kinase C isozymes, J. Am. Chem. Soc. 120 (1998) 9159–9167.
[16] K. Murakami, K. Irie, A. Morimoto, H. Ohigashi, M. Shindo, M. Nagao, T. Shimizu, T. Shirasawa, Synthesis, aggregation, neurotoxicity, and secondary structure of various Aβ1-42 mutants of familial Alzheimer's disease at positions 21–23, Biochem. Biophys. Res. Commun. 294 (2002) 5–10.

[17] Y. Masuda, K. Irie, K. Murakami, H. Ohigashi, R. Ohashi, K. Takegoshi, T. Shimizu, T. Shirasawa, Verification of the turn at positions 22 and 23 of the β-amyloid fibrils with Italian mutation using solid-state NMR, Bioorg. Med. Chem. 13 (2005) 6803–6809.
[18] W.L. Earl, Measurement of ^{13}C chemical shifts in solids, J. Mangn. Reson. 48 (1982) 35–54.
[19] J.L. White, L.W. Beck, D.V. Ferguson, J.F. Haw, Background suppression in MAS NMR, J. Magn. Reson. 100 (1992) 336–341.
[20] D.P. Raleigh, M.H. Levitt, R.G. Griffin, Rotational resonance in solid state NMR, Chem. Phys. Lett. 146 (1988) 71–76.
[21] R. Tycko, Molecular structure of amyloid fibrils: insights from solid-state NMR, Q. Rev. Biophys. 39 (2006) 1–55.
[22] O.N. Antzutkin, R.D. Leapman, J.J. Balbach, R. Tycko, Supramolecular structural constraints on Alzheimer's β-amyloid fibrils from electron microscopy and solid-state nuclear magnetic resonance, Biochemistry 41 (2002) 15436–15450.
[23] A. Morimoto, K. Irie, K. Murakami, Y. Masuda, H. Ohigashi, M. Nagao, H. Fukuda, T. Shimizu, T. Shirasawa, Analysis of the secondary structure of β-amyloid (Aβ42) fibrils by systematic proline replacement, J. Biol. Chem. 279 (2004) 52781–52788.
[24] D.M. Walsh, A. Lomakin, G.B. Benedek, M.M. Condron, D.B. Teplow, Amyloid β-protein fibrillogenesis. Detection of a protofibrillar intermediate, J. Biol. Chem. 272 (1997) 22364–22372.
[25] D.S. Wishart, C.G. Bigam, A. Holm, R.S. Hodges, B.D. Sykes, ^{1}H, ^{13}C and ^{15}N random coil NMR chemical shifts of the common amino acids. I. Investigations of nearest-neighbor effects, J. Biomol. NMR 5 (1995) 67–81.
[26] D.P. Raleigh, F. Creuzet, S.K. Das Gupta, M.H. Levitt, R.G. Griffin, Measurement of internuclear distances in polycrystalline solids: rotationally enhanced transfer of nuclear spin magnetization, J. Am. Chem. Soc. 111 (1989) 4502–4503.
[27] J.M. Griffiths, R.G. Griffin, Nuclear magnetic resonance methods for measuring dipolar couplings in rotating solids, Anal. Chim. Acta 283 (1993) 1081–1101.
[28] P.T. Lansbury Jr., P.R. Costa, J.M. Griffiths, E.J. Simon, M. Auger, K.J. Halverson, D.A. Kocisko, Z.S. Hendsch, T.T. Ashburn, R.G.S. Spencer, B. Tidor, R.G. Griffin, Structural model for the β-amyloid fibril based on interstrand alignment of an antiparallel-sheet comprising a C-terminal peptide, Nat. Struct. Biol. 2 (1995) 990–998.
[29] T. Lührs, C. Ritter, M. Adrian, D. Riek-Loher, B. Bohrmann, H. Döbeli, D. Schubert, R. Riek, 3D structure of Alzheimer's amyloid-β(1–42) fibrils, Proc. Natl. Acad. Sci. USA 102 (2005) 17342–17347.
[30] W. Hoyer, C. Grönwall, A. Jonsson, S. Ståhl, T. Härd, Stabilization of a β-hairpin in monomeric Alzheimer's amyloid-β peptide inhibits amyloid formation, Proc. Natl. Acad. Sci. USA 105 (2008) 5099–5104.
[31] A. Sandberg, L.M. Luheshi, S. Söllvander, T. Pereira de Barros, B. Macao, T.P. Knowles, H. Biverstål, C. Lendel, F. Ekholm-Petterson, A. Dubnovitsky, L. Lannfelt, C.M. Dobson, T. Härd, Stabilization of neurotoxic Alzheimer amyloid-β oligomers by protein engineering, Proc. Natl. Acad. Sci. USA 107 (2010) 15595–15600.
[32] H.A. Scheidt, I. Morgado, D. Huster, Solid-state NMR reveals a close structural relationship between amyloid-β protofibrils and oligomers, J. Biol. Chem. 287 (2012) 22822–22826.
[33] L.C. Serpell, Alzheimer's amyloid fibrils: structure and assembly, Biochim. Biophys. Acta 1502 (2000) 16–30.